Title: ZN148 – a modular synthetic metallo-β-lactamase inhibitor reverses carbapenem-resistance in Gram-negative pathogens *in vivo*

Running title: ZN148 - a synthetic metallo-β-lactamase inhibitor

Authors: Ørjan Samuelsen[a,b,1] (ORCID: 0000-0002-5525-2614), Ove Alexander Høgmoen Åstrand[c] (ORCID: 0000-0002-1490-9632), Christopher Fröhlich[a,d] (ORCID: 0000-0003-2682-2267), Adam Heikal[e] (ORCID: 0000-0002-5604-7145), Susann Skagseth[d], Trine Josefine Olsen Carlsen[d], Hanna-Kirsti S. Leiros[d] (ORCID: 0000-0002-2726-6322), Annette Bayer[f] (ORCID: 0000-0003-3481-200X), Christian Schnaars[c], Geir Kildahl-Andersen[c], Silje Lauksund[a,b], Sarah Finke[e], Sandra Huber[g], Tor Gjøen[e], Adriana Magalhaes Santos Andresen[e], Ole Andreas Økstad[e] (ORCID: 0000-0001-9351-8535), Pål Rongved[c,1] (ORCID: 0000-0001-6678-1952)

Author Affiliations: [a]Norwegian National Advisory Unit on Detection of Antimicrobial Resistance, Department of Microbiology and Infection Control, University Hospital of North Norway, Tromsø, Norway. [b]Department of Pharmacy, UiT The Arctic University of Norway, Tromsø, Norway. [c]Section for Pharmaceutical Chemistry, Department of Pharmacy, University of Oslo, Oslo, Norway. [d]The Norwegian Structural Biology Centre (NorStruct), UiT The Arctic University of Norway, Tromsø, Norway. [e]Centre for Integrative Microbial Evolution (CIME) and Section for Pharmacology and Pharmaceutical Biosciences, Department of Pharmacy, University of Oslo, Blindern, Oslo, Norway. [f]Department of Chemistry, UiT The Arctic University of Norway, Tromsø, Norway. [g]Department of Laboratory Medicine, Division of Diagnostic Services, University Hospital of North Norway, Tromsø, Norway.

[1] To whom correspondence may be addressed: E-mail: orjan.samuelsen@unn.no or pal.rongved@farmasi.uio.no

Abstract:

Carbapenem-resistant Gram-negative pathogens are a critical public health threat and there is an urgent need for new treatments. Carbapenemases (β-lactamases able to inactivate carbapenems) have been identified in both serine β-lactamase (SBL) and metallo β-lactamase (MBL) families. The recent introduction of SBL carbapenemase-inhibitors has provided alternative therapeutic options. Unfortunately, there are no approved inhibitors of MBL-mediated carbapenem-resistance and treatment options for infections caused by MBL-producing Gram-negatives are limited. Here, we present ZN148, a zinc-chelating MBL-inhibitor capable of restoring the bactericidal effect of meropenem and *in vitro* clinical susceptibility to carbapenems in >98% of a large international collection of MBL-producing clinical *Enterobacterales* strains (n=234). Moreover, ZN148 was able to potentiate the effect of meropenem against NDM-1-producing *Klebsiella pneumoniae* in a murine neutropenic peritonitis model. ZN148 showed no inhibition of the human zinc-containing enzyme glyoxylase II at 500 µM and no acute toxicity was observed in an *in vivo* mouse model with cumulative dosages up to 128 mg/kg. Biochemical analysis showed a time-dependent inhibition of MBLs by ZN148 and removal of zinc ions from the active site. Addition of exogenous zinc after ZN148 exposure only restored MBL activity by ~30%, suggesting an irreversible mechanism of inhibition. Mass-spectrometry and molecular modelling indicated potential oxidation of the active site Cys221 residue. Overall, these results demonstrate the therapeutic potential of a ZN148-carbapenem combination against MBL-producing Gram-negative pathogens and that ZN148 is a highly promising MBL inhibitor, capable of operating in a functional space not presently filled by any clinically approved compound.

Introduction:

The global increase in antimicrobial resistance is currently undermining our ability to treat bacterial infections and has become a critical public health threat worldwide. A cornerstone treatment of serious and life-threatening infections caused by multidrug-resistant (MDR) Gram-negative bacterial pathogens such as *Klebsiella pneumoniae* and *Escherichia coli* has been the carbapenem β-lactam antibiotics (e.g. meropenem) (1). The major advantage of carbapenems has been their relative stability towards β-lactamases, such as the extended-spectrum β-lactamases (ESBLs) and AmpCs, which constitute common resistance mechanisms against β-lactams (2). However, we now observe a global increase in dissemination and diversity of β-lactamases (carbapenemases) with the ability to inactivate carbapenems (3). Estimates indicate that carbapenem-resistant *E. coli* and *K. pneumoniae* caused around 3.6 million bloodstream or other serious infections globally in 2014 (4). The impact of carbapenem-resistance is further illustrated in a European study where carbapenem-resistance was shown to be the major contributor to the burden of infections by antibiotic-resistant bacteria in many countries (5). Moreover, a common feature of carbapenemase-producing Gram-negative bacteria is MDR, including resistance towards non-β-lactam antimicrobials, resulting in severely limited treatment options (6).

β-Lactamases are divided into two main families and four classes, the serine β-lactamases (SBLs, class A, C and D) and the metallo-β-lactamases (MBLs, class B) (2). The main distinction between SBLs and MBLs is that SBLs possess an active site serine, while MBLs require the presence of zinc ions for activity. β-lactamases with carbapenemase activity have been identified in both of these families including SBLs such as KPC and OXA-48-like, and the MBLs NDM, VIM and IMP (2). The recent introduction of serine carbapenemase inhibitors such as avibactam, vaborbactam and relebactam used in combination with β-lactams, have provided

72 treatment options against serine carbapenemase-producing Gram-negative pathogens (7, 8).
73 Unfortunately, none of these β-lactamase inhibitors possess inhibitory activity against MBLs.
74 The recent Italian outbreak of NDM-producing *Enterobacteriaceae* is significant due not only to
75 its size but also the change in epidemiology of carbapenem-resistant *Enterobacteriaceae* (CRE)
76 from endemic KPC-producing CRE to NDM-producing CRE and the subsequent reduction in
77 treatment options (9). Consequently, new treatment options for infections caused by MBL-
78 producing Gram-negatives, including NDM-producing *Enterobacterales*, are urgently required.

79 Possible treatment options includes cefiderocol (10) and the combination aztreonam-
80 avibactam (11, 12). Combinations of β-lactams and β-lactam enhancers such as zidebactam (13)
81 and nacubactam (14) have also shown promising activities. Moreover, several MBL inhibitors,
82 including aspergillomarasmine A (15), dipicolinic acid derivatives (16), ANT431 (17),
83 bisthiazolodines (18) and bismuth antimicrobials (19) have been reported. Recently, VNRX-
84 5133 (taniborbactam), a dual SBL and MBL inhibitor have shown potent activity in combination
85 with cefepime against MBL-producers (20). However, no direct MBL inhibitors are approved for
86 clinical use (21). Here, we report the pre-clinical development and characterization of a synthetic
87 and modular MBL-inhibitor (ZN148) with promising *in vitro* and *in vivo* efficacy.

88

89 **Results and discussion:**

90 **Synthesis of ZN148.** ZN148 is a construct of the zinc chelator tris-picolylamine (TPA) (22)
91 covalently linked to meglumine, a hydrophilic glucosyl side chain, through an *N*-methylated
92 amide bond, in order to lower the lipophilicity and toxicity of the chelator-conjugate (Fig. 1).
93 TPA is a known lipophilic zinc chelator with high affinity (10^{11} M) towards Zn^{2+} and has
94 previously been shown to inhibit MBLs (23-26). Synthesis of ZN148 is achieved through a high-

yield, 3-step synthesis from commercially available building blocks (Fig. S1), and the compound exhibits very high aqueous solubility (1.225 g/mL in phosphate buffered saline).

***In vitro* activity of ZN148.** Unmodified TPA re-sensitized NDM-1-producing *K. pneumoniae* and VIM-2-producing *P. aeruginosa* clinical isolates towards meropenem by reducing the minimum inhibitory concentration (MIC) from 32-64 mg/L to 0.125 and 1 mg/L, respectively (Table S1). However, TPA also demonstrated a high degree of toxicity against human hepatocarcinoma (HepG2) cells (IC_{50} 9.8 µM). In contrast, ZN148 displayed not only a comparatively reduced toxicity against HepG2 cells (IC_{50} >100 µM), which is most likely due to its much lower cell permeability, but also retained the potentiation of meropenem activity and fully restored meropenem clinical susceptibility according to EUCAST clinical breakpoints (27) when tested at 50 µM against the same isolates (Table S1). This indicates that ZN148 is able to penetrate the Gram-negative cell wall and enter the periplasm where the MBLs are located. Alternatively, ZN148 could lower the environmental pool of available zinc, decreasing periplasmic zinc and consequently the activity of MBLs (28). ZN148 exhibited no intrinsic antibacterial activity at concentrations up to 500 µM, confirming that the potentiation of meropenem is not due to combined antibacterial activity of the compounds.

ZN148 at 50 µM was further tested in combination with meropenem against an extended international collection of 234 MBL-producing clinical *Enterobacterales* strains expressing variants of NDM, VIM and IMP enzymes as well as other non-MBL β-lactamase variants. Overall, the meropenem-ZN148 combination reduced the meropenem MIC to susceptible levels (≤ 2 mg/L) in >98% of strains (MIC_{90} meropenem: ≥64 mg/L and MIC_{90} meropenem-ZN148: 0.5 mg/L) (Fig. 2A, and Table S2). The geographical distribution and diversity of the strain

collection shows that ZN148 is not influenced by strain background or specific MBL-variants. Similarly, when tested against a subset of 173 MBL-producing *E. coli* and *K. pneumoniae*, ZN148 reduced the doripenem and imipenem MIC to susceptible levels in >99% of strains (Fig. 2B) indicating a potential to be used in combination with other carbapenems. Against MBL-producing *P. aeruginosa* (*n*=52) and *A. baumannii* (*n*=6) strains, ZN148 exhibited less potentiation of carbapenems, though still restored clinical susceptibility in 17%, 15% and 25% of MBL-producing *P. aeruginosa* clinical strains in combination with meropenem, doripenem or imipenem, respectively (Fig. 2C). Against NDM-1-producing class D carbapenemase-negative *A. baumannii* strains, ZN148 reduced the meropenem MIC >2-fold in 4/6 clinical strains (Table S3). The cause of the reduced effectiveness against *P. aeruginosa* and *A. baumannii* isolates is not clear, but could be due to a more restricted outer membrane permeability than in *Enterobacterales* (29). This could reduce the uptake of carbapenems or ZN148, and/or a range of efflux systems which could contribute to carbapenem-resistance particularly in *P. aeruginosa* (30). Alternatively, if ZN148's mode of action is through lowering the environmental availability of zinc, differential zinc uptake between *Enterobacterales* and *A. baumannii*/*P. aeruginosa* could be involved.

With a few exceptions, no potentiation of meropenem, doripenem and imipenem was observed in strains co-producing MBLs and class D carbapenemases (Table S4). Further, no potentiation of meropenem, doripenem or imipenem was observed for ZN148 against strains harboring only the class A carbapenemase KPC (Table S5), supporting the specificity towards MBLs.

A time-dependent cell-killing assay revealed that ZN148 restored the bactericidal activity of meropenem against an NDM-1-producing *K. pneumoniae* strain (Fig. 3). Meropenem alone (4

mg/L) produced an initial bacteriostatic effect (2-log reduction in cell numbers), before eventually reaching >1x10^9 colony forming units per milliliter (CFU/mL) after 24 hours. In contrast, the combination of meropenem (4 mg/L) with either 50 or 100 μM ZN148 was bactericidal, restoring a time-dependent killing mechanism. The kinetics of killing were similar for both concentrations of ZN148 tested. Cell numbers were reduced to below the limit of detection (1x10^2 CFU/mL) after 8 hours and no re-growth was observed within 24 hours, indicating sterilizing bactericidal activity.

Following an investigation into the frequency of resistance (FoR) using single step selection, we observed a concentration dependent reduction in FoR for both meropenem and ZN148 (Table S6), with the FoR ranging between 10^{-7} to 10^{-8} using an NDM-1-producing *K. pneumoniae* strain (K66-45). Whole genome shotgun sequencing (WGS) of stable, isolated mutants revealed mutations within the outer membrane porin OmpK36 (locus tag: B5G58_03310) and a LysR type transcriptional regulator (locus tag: B5G58_25480) previously associated with changes in OmpC expression in *E. coli* (Table S7) (31). Serial passaging of *K. pneumoniae* K66-45 against increasing concentrations of meropenem, in the presence of 50 and 100 μM ZN148 resulted in 64x and 16x fold increase in MIC, respectively, compared to the control culture (Fig. S3). WGS analysis of stable mutants isolated from the 100 μM ZN148 serial-passaging condition (isolated at 16-fold meropenem MIC, 2 mg/L) also identified mutations in OmpK36 and the same LysR type transcriptional regulator as from the single step selection (Table S8). Evolution of NDM have shown the emergence of allelic variants with enhanced zinc binding capability and increased ability to tolerate zinc starvation caused by metal chelators (32). However, no mutations were observed in the bla_{NDM-1} gene in either spontaneous (single-step) or serially passaged mutants emerging during exposure to ZN148, and no mutants

reached clinical resistance levels. Taken together, these results demonstrated that development of resistance to ZN148 and meropenem co-treatment is unlikely to be a barrier to further development of ZN148 as an MBL inhibitor.

ZN148 potentiates the activity of meropenem *in vivo* with no acute toxicity *in vivo.* In a murine neutropenic peritonitis model, subcutaneous treatment with a combination of meropenem (33 mg/kg) and ZN148 (10 mg/kg) resulted in a significantly lower CFU/mL of a meropenem-resistant NDM-1-producing *K. pneumoniae* strain in both peritoneal fluid ($p<0.0001$) and blood ($p<0.01$), compared to treatment with meropenem alone (Fig. 4). Treatment with ZN148 alone did not result in a reduction of CFU compared to vehicle treatment, corroborating the lack of intrinsic antibacterial activity observed *in vitro*. The same effect was observed for 33 and 100 mg/kg ZN148 (Fig. S2).

As zinc is an essential metal ion for many biological processes (33, 34), inhibitors of MBLs based on zinc chelation could potentially have off-target toxicity. To investigate this, we tested the inhibitory activity of ZN148 against the human glyoxylase II enzyme, which shares the MBL-protein fold and zinc-binding properties (35). In contrast to EDTA, a strong metal chelator, ZN148 (500 µM) showed no inhibitory activity against recombinant glyoxylase II (Fig. 5A). This indicates selectivity towards bacterial MBLs and a more specific mode of action. Selectivity towards bacterial MBLs has also been shown for other zinc-chelating MBL inhibitors such as aspargillomarasmine A (15). Moreover, the inhibitory activity of ZN148 was not influenced by human serum albumin and α_1-acid glycoprotein, indicating negligible serum protein binding (Fig. S4). Additionally, no acute toxicity was observed *in vivo* in a maximum tolerated dose study using female Balb/C mice. In four groups, containing twelve animals each, after weekly

doubling of single doses from 4 mg/kg up to 128 mg/kg and a 7-week cumulative administration of 252 mg/kg, no significant differences in clinical signs (hair loss or bristly hair, immobility, prostration) or loss of weight (<10% as compared to initial weight) (Fig. 5B) were observed between the test and control groups.

ZN148 irreversibly inhibits MBLs. The rationale behind inclusion of the TPA moiety in ZN148 was to inhibit MBLs by the removal of their active site zinc ions. Using ICP-MS for analysis of purified VIM-2 and NDM-1, we found that ZN148 removed ~1.8 molar and ~1.3 molar equivalents of zinc from VIM-2 and NDM-1, respectively (Fig. 6A). We also synthesized three ZN148 analogues, ZN222, ZN223 and ZN228, where one or several 2-pyridinyl rings were replaced with benzene rings, resulting in reduced chelator strength (23). Analysis of NDM-1 and VIM-2 enzyme kinetics revealed that the inhibitory efficiency (k_{inact}/K_i) of these compounds was lower than for ZN148 and correlated with the theoretical chelator strength (Table 1). The relative position of the pyridine- and benzene rings in the ZN148 derivatives (ZN223 and ZN228) affected the inhibitory activity (Table 1). However, none of the ZN148 analogues were able to potentiate meropenem activity towards an NDM-1-producing *K. pneumoniae* or a VIM-2-producing *P. aeruginosa* strain, i.e. the meropenem MIC was unchanged (32 mg/L) both alone and in combination with ZN222, ZN223 or ZN228, confirming that zinc chelation is required for activity and constitutes the likely mode of inhibition for ZN148.

In vitro inactivation kinetics revealed that ZN148 inhibited VIM-2 (k_{inact}/K_i: 6.6 min^{-1} mM^{-1}) more effectively than NDM-1 (k_{inact}/K_i: 0.19 min^{-1} mM^{-1}) and showed a time-dependent inhibition of VIM-2 and NDM-1 by ZN148 (Table 1), suggestive of an irreversible mechanism of inhibition (36, 37). Following incubation of VIM-2 with ZN148, addition of exogenous zinc

restored only ~30% of the MBL activity compared to the untreated control (Fig. 6B). Unfolding and step-wise refolding of VIM-2 following incubation with ZN148 also resulted in restoration of ~30% of the control activity (Fig. 6C). In contrast, incubation of VIM-2 with EDTA followed by addition of zinc resulted in complete, or near complete (~80%) restoration of activity (Fig. 6B and 6C). Taken together, these results demonstrate a difference in the mode of inhibition for ZN148 compared to EDTA, and support an irreversible mechanism of inhibition of VIM-2 by ZN148. The mechanism behind the irreversible inhibition is unclear, but several studies have postulated that chelating agents increase the susceptibility of active site amino acids to chemical modifications, such as oxidation of Cys221 to Ocs221 (38-40). ESI-MS analysis of purified VIM-2 incubated with ZN148 revealed an increase in mass of 46.2±0.1Da (25,572.7±0.1 Da to 25,618.9±0.1 Da) (Fig. 6D), potentially representative of a deprotonated cysteine sulfonic acid (47 Da). The observed mass increase indicates that removal of zinc by ZN148 renders the enzyme more susceptible to irreversible chemical modification (e.g. oxidation of Cys221) (38, 39, 41), thus preventing the restoration of enzymatic activity by refolding upon addition of exogenous zinc.

Molecular modeling of ZN148 into the active sites of VIM-2 (PDB ID: 5LSC) and NDM-1 (PDB ID: 4RL0) predicted favorable aromatic interactions between ZN148 and F61, Y67, and Y224 and cation-pi interactions to R228 in VIM-2 (Fig. 6E). The stacking of these aromatic side chains would likely favor greater hydrophobic and cation-pi interactions of ZN148 with the VIM-2 active site compared to the equivalent residues (M61, V67, K224 and A228) in NDM-1. ZN148 in NDM-1 would then have fewer enzyme-inhibitor interactions (Fig. 6F), and a less favorable ZN148 binding compared to VIM-2 (Table 1). This could indicate formation of a transient enzyme:Zn:inhibitor complex followed by the removal of zinc ions from the active site

Antimicrobial Agents and Chemotherapy

as shown for several other MBL inhibitors (42). The inactivated Zn-depleted VIM-2 enzyme demonstrated an increased mass of +46.2±0.1 Da, which is likely due to the oxidation of Cys221, since oxidation to Ocs221 is observed more often in VIM (40, 43, 44) than in NDM-1 crystal structures. Second shell residues, fold or zinc affinity might also account for an easier Cys221 oxidation in VIM-2 compared to NDM-1.

Conclusions. The lack of available therapies for infections caused by MBL-producing Gram-negative bacteria has prompted the World Health Organization to classify them as 'priority pathogens' for research and development of new and effective treatments (45). Discovery and development of new antibiotics is fraught with difficulty and suffers from high attrition rates at early stages of development (46). The successful clinical introduction of SBL-carbapenemase inhibitors demonstrated an alternative strategy, preserving the efficacy of existing antibiotics - however, this success has not to date been replicated in the treatment of MBL-producing CRE.

To meet the challenge posed by MBL-producing CRE, we adopted a strategy of developing a synthetic, module zinc-chelator. Taken together, the activity spectrum of ZN148 in combination with carbapenems, *in vivo* efficacy and limited *in vivo* toxicity demonstrate that ZN148 has the potential to enter pre-clinical studies for further development. Furthermore, as a modular and easy-to-synthesize MBL inhibitor that restores the activity of carbapenems towards a range of clinically important Gram-negative MDR pathogens, ZN148 is well placed to enter the clinical development pipeline along with other promising recently approved molecules (47) in meeting the urgent, therapeutic challenge of global importance.

Materials and Methods:

The chemical synthesis of ZN148 and analogues ZN222, ZN223 and ZN228 is described in the Supplemental material and Fig. S1.

Solubility measurements of ZN148 in phosphate buffered saline (PBS):

The solubility of ZN148 was evaluated in PBS buffer at pH 7.4. Increasing amounts of ZN148 was dissolved in 1.0 mL at room temperature by gentle swirling of the solution in a glass vial. A total of 1.225 g ZN148 was successfully dissolved in 1.0 mL PBS buffer, giving a total volume of 1.8 mL. This solution was stable at 4°C for more than 6 weeks without precipitation.

Antibacterial susceptibility testing and time-kill experiments:

Minimum inhibitory concentrations (MICs) of carbapenems alone and in combination with inhibitors were determined by broth microdilution according to the Clinical and Laboratory Standards Institute (CLSI) guidelines (48) either using pre-made plates (TREK Diagnostic Systems/Thermo Fisher Scientific, East Grinstead, UK) with meropenem or in-house prepared plates with meropenem, imipenem and doripenem. ZN148 and other inhibitors were tested at a fixed concentration of 50 µM. Cation-adjusted Mueller Hinton medium (TREK Diagnostic Systems/Thermo Fisher Scientific, East Grinstead, UK/Becton-Dickinson, Franklin Lakes, NJ, USA) were used as growth medium. The plates were incubated for 20 h at 37°C. ZN148, ZN222, ZN223, ZN228 and TPA were initially tested in combination with meropenem using two indicator strains, one NDM-1-producing *K. pneumoniae* (49, 50) and one VIM-2-producing *P. aeruginosa* (51). The activity of ZN148 were subsequently tested against two extended strain collections: (i) in combination with meropenem against MBL-producing *Enterobacterales* (*n*=62), MBL-producing *P. aeruginosa* (*n*=9) and MBL- and class D carbapenemase co-producing *Enterobacterales* (*n*=5) from the strain collection at the Norwegian National Advisory

Unit on Detection of Antimicrobial Resistance, Norway and (ii) in combination with meropenem, imipenem and doripenem against globally collected MBL-producing *E. coli* (*n*=87), *K. pneumoniae* (*n*=85), *P. aeruginosa* (*n*=52) and *A. baumannii* (*n*=6), MBL- and class A/D carbapenemase co-producing *E. coli* (*n*=11), *K. pneumoniae* (*n*=15) and *A. baumannii* (*n*=7) at IHMA Europe Sàrl, Switzerland. *E. coli* ATCC 25922 and *P. aeruginosa* ATCC 27853 were used as quality control strains. The MBL inhibitors were also tested for intrinsic antibacterial activity against the strains.

To determine the kinetics of killing of the meropenem-ZN148 combination, NDM-1-producing *Klebsiella pneumoniae* K66-45 ($1x10^6$ CFU/mL) in cation-adjusted Mueller Hinton broth II (Sigma-Aldrich, St. Louis, USA) was treated with either 4 mg/L meropenem or a combination of 4 mg/L meropenem plus 50 or 100 µM ZN148 and grown at 37°C with shaking (180 r.p.m.). Cell number was determined over the course of 24 h by a modified Miles-Misra method (52). Briefly, 10 mL serial dilutions of culture in sterile phosphate buffered saline (PBS) were spotted and dried on square (10cm x 10cm) Luria-Bertani agar (Oxoid, Basingstoke, UK) plates at room temperature before incubation at 37°C. Limit of detection was set as two colonies in 10 mL undiluted culture, representing 100 CFU/mL.

***In vivo* efficacy study:**

The *in vivo* efficacy of meropenem (Mylan, Mylan Hospitals, Asker, Norway) in combination with ZN148 were evaluated in a murine neutropenic peritonitis model. Female NRMI mice **(**Taconic Biosciences, Lille Skensved, Denmark**)** were rendered neutropenic by intraperitoneal (i.p.) injection with cyclophosphamide (Baxter, Søborg Denmark) at four days (200 mg/kg) and

one day (100 mg/kg) prior to inoculation. Mice were inoculated i.p. with ~5x10^6 CFU of NDM-1-producing *K. pneumoniae* 50752501. One hour post-inoculation mice were injected subcutaneously (s.c.) in the neck region with ZN148 corresponding to 10, 33 and 100 mg/kg or vehicle. 30 min later the mice were injected s.c. with 33 mg/kg meropenem or vehicle. Four mice were included for each treatment regime. Five hrs post-inoculation the mice were anesthetized and blood was collected from axillary cutdown and the mice were sacrificed. Subsequently, two ml sterile saline was injected i.p. and intraperitoneal fluid was sampled. Blood and intraperitoneal fluid were serially diluted in 0.9% NaCl and plated on blood agar plates with 5% horse blood (Statens Serum Institut, Copenhagen, Denmark) for CFU determination. Groups were analyzed with ANOVA Dunnett´s multiple comparisons test in GraphPad Prism 7.04 (GraphPad Software Inc, USA). *P*-values <0.05 were considered statistically significant. All animal experiments were approved by the National Committee of Animal Ethics, Denmark (permission no. 2014-15-0201-00171) and adhered to the standards of EU Directive 2010/63/EU.

Single-step selection of *K. pneumoniae* K66-45 for growth on meropenem and ZN148 in combination:

In order to determine the frequency of resistance to the combination of meropenem and ZN148, a modified single-step selection experiment was carried out as previously described (53). Briefly, NDM-1-producing *K. pneumoniae* K66-45 was grown from a single colony to approximately 10^9 CFU/ml and plated on cation-adjusted Mueller-Hinton broth II (Becton Dickinson, Franklin Lakes, NJ USA) agar containing 30, 50, 100 or 200 μM ZN148 and 0.5, 1, 2, 4 or 8 mg/L meropenem, in combination. Colonies were counted after overnight incubation at 37 °C. The concentrations of meropenem chosen ranged from 4x to 64x MIC (MIC values in the absence of

ZN148) and correlated with EUCAST clinical breakpoints for *Enterobacterales*, which define ≤2 mg/L as sensitive and >8 mg/L as resistant to meropenem (18).

Serial passaging of *K. pneumoniae* K66-45:

K. pneumoniae K66-45 was passaged in a 96-well microtiter plate with a consistent concentration of ZN148 and increasing concentrations of meropenem. To start the passaging cation-adjusted Mueller Hinton Broth II medium (Sigma-Aldrich) containing 0.0625 mg/L (0.5 x MIC) and 50 or 100 µM of ZN148 was inoculated with 1% of overnight culture which was grown without selection. Six biological replicates were passaged in parallel, and from each of the six overnight cultures four wells were inoculated, resulting in 24 subcultures for each ZN148 concentration. After 24 hours of incubation at 37 °C and shaking at 180 rpm, the wells were visually checked for growth. Passaging was continued with all subcultures showing growth by transferring 1 µl to 100 µl of fresh medium added 0.125 mg/L meropenem (1 x MIC) and 50 or 100 µM of ZN148, respectively. This process was continued by increasing the meropenem concentration by 2-fold every 24 hours until none of the subcultures showed growth.

DNA preparation and *de novo* whole genome sequencing of evolved clones from single-step selection and serial passaging experiments:

Preparation of genomic DNA from NDM-1 producing *K. pneumoniae* K66-45 was carried out using the MO BIO DNeasy UltraClean Microbial kit (Qiagen, USA) as previously described (49). Whole genome shotgun (WGS) sequencing was carried out at either the Norwegian Sequencing Centre (Oslo, Norway) or Novogene (Beijing, China) using the Illumina HiSeq platform. Variations and single nucleotide polymorphisms in mutant WGS sequences with

348 greater than 10x coverage were identified by mapping Illumina reads to the reference genome
349 (GenBank accession numbers CP020901 – CP020905) (49) using Bowtie2 (54) within Geneious
350 version 11.1.5 (55) and using the inbuilt Geneious variant/SNP finder command.
351
352 ***In vitro* toxicity:**
353 The human hepatoblastoma cell line HepG2 (HB-8065, ATCC, Manassas, VA, USA) was
354 cultured in DMEM-Glutamax™ (5.5 mM glucose, ThermoFisher, USA) supplemented with 10%
355 fetal bovine serum (Sigma-Aldrich, USA), streptomycin (100 µg/ml, Gibco/ThermoFisher, USA)
356 and penicillin (100 units/ml, Gibco/ThermoFisher, USA) at 37 °C in 5% CO_2. For viability
357 assays, cells were seeded in white 96-well Nunclon plates (Sigma-Aldrich, USA) at a density of
358 20000 cells/well and left overnight to adhere. ZN148 and TPA (Sigma-Aldrich, Darmstadt,
359 Germany) dissolved in DMSO (Sigma-Aldrich, USA) were added to the white 96-well plates
360 containing 20000 HepG2 cells/well at concentrations ranging from 1 to 1 x 10^{-3} mM (DMSO
361 concentration kept below 1%) and incubated for 24 hours at 37°C in 5% CO_2. After 24 hours,
362 AlamarBlue cell viability reagent (Thermo Fisher, Carlsbad, USA) was added (10% final
363 concentration) and incubated for 4 hours at 37°C. The proportion of viable cells in each well
364 was measured in a fluorescence plate reader (Clariostar, BMGlabtech, Germany) at ex550
365 nm/em603 nm (56). Data from eight replicates were fitted by non-linear regression to determine
366 IC_{50} values using GraphPad Prism (GraphPad Software Inc, USA).
367
368 ***In vivo* tolerance:**
369 *In vivo* tolerance of ZN148 was performed by Antineo (www.antineo.fr). Female Balb/c mice (4
370 weeks old, approximately 20 g, Charles River, L'Arbresle, France) were acclimatized 4 days in

the animal facility before initiation of experiments. Groups of six mice were either untreated or treated with 200 µL ZN148 (0.4-12.8 g/L) intraperitoneally once a week. Doses were doubled each week (4-128 mg/kg) in the absence of any observed weight loss or modification in behaviour. Individual weights were followed four days a week. Relative weight was calculated as the ratio between the weight of the day and the weight at the initiation of the experiment. Animals were also followed for macroscopic modifications in behavior. The protocol for experiments in mice was approved by the University of Lyon Animal Ethics Committee (Comité d'Ethique en Expérimentation Animale de l'Université Claude Bernard Lyon 1, authorization number DR2015-09).

Protein binding:

Protein binding of ZN148 were investigated using the Transil^{XL} plasma protein binding kit (Sovicell, Leipzig, Germany) containing human serum albumin and α_1-acid glycoprotein in a ratio of 24:1. 500 µM ZN148 in 50 mM HEPES buffer, pH 7.5 were added to different concentrations (0–140 µM) of the protein mixture and incubated for 12 min at room temperature with shaking at 1200 rpm. After incubation, the suspensions were centrifuged for 5 min on a Minifuge (Starlab, Milton Keynes, UK) and the supernatant was diluted 1:10 in 50 mM HEPES buffer, pH 7.5 supplemented with 1 µM $ZnSO_4$ (Sigma Aldrich, St. Louis, USA). VIM-2 was added at final concentration of 1 nM and the solution was incubated for 10 and 30 min at 25°C. The enzyme activity was measured by adding nitrocefin (Merck, Darmstadt, Germany) at a final concentration of 50 µM and measured at 482 nm at 25°C in a SpectraMax Plus plate reader (Molecular Devices). Buffer alone was included as a control.

Interaction with human glyoxylase II:

Recombinant human glyoxylase II (rHGly II, R&D systems, USA) was incubated with and without ZN148 (final concentrations of 125, 250 and 500 µM) for 10 and 30 min at 25°C in 50 mM Tris buffer (Merck, Darmstadt, Germany) supplemented with 250 mM NaCl, pH 7.5. 50 µL of substrate mixture containing 2 mM S-Lactoylglutathione and 400 µM 5,5`-dthiobis(2-nitrobenzoic acid (Sigma Aldrich, St. Louis, USA) were mixed together with 50 µL of the pre-incubated rHGly II at a final enzyme concentration of 0.2 ng/µL. The initial enzymatic velocity was measured at 405 nm in 96 well plates (Thermo Fisher Scientific, Roskilde, Denmark Nunc) at 25°C in a SpectraMax Plus plate reader (Molecular Devices). EDTA (Merck, Darmstadt, Germany) was included as a control.

Time-dependent inactivation kinetics:

Protein expression and purification of NDM-1 and VIM-2 was done as previously described (36, 43, 57). Stock solutions of purified NDM-1 and VIM-2 were prepared in 50 mM HEPES buffer (Merck, Darmstadt, Germany), pH 7.5. Inhibition of NDM-1 and VIM-2 were determined for ZN148 and the analogues ZN222, ZN223 and ZN228 at different concentrations of inhibitor after pre-incubation times of 2, 8, 15, 25 and 32 min in 50 mM HEPES buffer pH 7.5 supplemented with 1 µM $ZnSO_4$ (Sigma Aldrich, St. Louis, USA) and bovine serum albumin (BSA, Sigma Aldrich, St. Louis, USA, final concentration 2 µg/mL) at 25°C. A concentration of 1 nM VIM-2 and 30 nM NDM-1 were used and the reaction was initiated by the addition of 30 µM nitrocefin (Merck, Darmstadt, Germany) for VIM-2 or 100 µM imipenem (Sigma Aldrich, St. Louis, USA) for NDM-1. The reaction was measured at 482 nm (VIM-2) or 300 nM (NDM-1) in either standard 96 well plates (Thermo Fisher Scientific, Roskilde, Denmark) for VIM-2 or

417 UV-transparent 96 well plates (Corning, Kennebunk, ME, USA) for NDM-1 at 25°C in a
418 SpectraMax Plus plate reader (Molecular Devices). All enzyme and substrate concentrations
419 indicated are final concentrations in the assay. The enzyme activity in percent was calculated
420 based on the initial velocity and compared to the control without inhibitor compound. All tests
421 were performed at least in duplicates.
422
423 The observed rate constant (k_{obs}) per inhibitor concentration was calculated from the slope of
424 semilog plot of enzyme activity in % *versus* preincubation time. The individual values of k_{obs}
425 were plotted against the inhibitor concentration and saturation kinetics were fitted into Eq. 1 by
426 using Graph Pad Prim 4 (GraphPad Software Inc, USA) based on the following model:
427
428 $$E\bullet Zn + I \overset{K_I}{\leftrightarrow} E\bullet Zn\bullet I \xrightarrow{k_{inact}} E + Zn\bullet I \text{ and } E^*\bullet Zn\bullet I$$
429
430 where K_I represents the inhibitor concentration that leads to an half-maximum inactivation of the
431 enzyme, k_{inact}, states the first-order rate constant, $E\bullet Zn^{2+}$, the holoenzyme, I, the inhibitor,
432 $E\bullet Zn\bullet I$, the enzyme:Zn:inhibtior ternary complex, E, inactive Zn-depleted enzyme, $Zn\bullet I$, the
433 zinc-inhibitor complex and $E^*\bullet Zn\bullet I$, the inactive enzyme:Zn:inhibitor ternary complex (39).
434
$$k_{obs} = \frac{k_{inact}\,[I]}{\frac{[S]}{K_I} + [I]} \qquad (1)$$
435
436 By fitting these values, the irreversible kinetic parameters maximum inactivation rate (k_{inact}) and
437 the inhibitor concentration that produces half-maximal rate of inactivation (K_I) were obtained.

Finally, the inhibitors were characterized by calculating k_{inact}/K_I. Where no saturation curve could be observed, K_I and k_{inact} were determined from the linear part of plot $1/k_{obs}$ *versus* 1/[I].

Zinc^{66} determination by inductively coupled plasma mass spectrometry (ICP-MS):

ICP-MS was used to investigate the chelating property of ZN148 by measuring the zinc concentration (Zn^{66}) after incubation of VIM-2 with and without ZN148 in zinc depleted 50 mM HEPES buffer (chelex HEPES buffer), pH 7.5. The chelex buffer were prepared by stirring 2 g chelex resin (Bio-Rad, Hercules, USA) in 100 mL 50 mM HEPES buffer, pH 7.5. The resin was subsequently removed by sterile filtration (Merck MilliPore, 0.22 µm). VIM-2 (10 g/L) was diluted to 12.5 mg/L and mixed with ZN148 at different final concentrations (0, 12.5, 125 and 1250 µM) in chelex HEPES buffer. All solutions were allowed to incubate for 30 min on ice and subsequently concentrated by centrifugation (at 4,000 x g, 4°C for 25 min) to a volume of 250 µL using centrifugal molecular cut-off filters (Merck MilliPore, 10,000 Da). The residual inhibitor within these samples was diluted by factor of 5,000 using the same type molecular cut-off filters and 50 mM chelex HEPES buffer, pH 7.5. The VIM-2 protein was concentrated to 0.2 g/L followed by a 1/16 dilution with 750 µL of a diluent mixture containing Rh^{103} (Inorganic Ventures, Christiansburg, VA, USA) as internal standard. The diluent mixture consisted of Milli-Q water (Millipore/ Merck KGaA, Darmstadt, Germany) with 2 µg/ Rh^{103}, 2.5% v/v ammonia solution (Honeywell Fluka, Bucharest, Romania), 0.08% v/v Triton X-100 (Sigma/Merck KGaA, Darmstadt, Germany), 10% v/v isopropanol (Honeywell Fluka, Bucharest, Romania) and 0.25 µg/L Au (Inorganic Ventures, Christiansburg, VA, USA) as stabiliser. The samples were introduced to the nebulizer (N2 gas flow 1.03 mL/min) by an ESI-Fast SC2DX autosampler with a sample flow rate of 3 rpm and further into the NexION 300D ICP-MS system (Perkin Elmer,

Waltham, MA, USA). Per inhibitor concentration of at least three biological replicates were performed and injected and measured in triplicates. For the MS analysis the kinetic energy discrimination (KED) mode with a helium flow rate of 5.7 mL/min, 20 sweeps per reading and a dwell time of 100 ms/AMU for Zn^{66} and 50 ms/AMU for Rh^{103} were applied. The measurements were performed with following instrumental settings: rf power (1,600 W), plasma gas flow (18 mL/min Ar), auxillary gas flow (1.2 mL/min N2), RPQ voltage (0.25 V) integration time (2,000 ms). All zinc concentrations were obtained by the internal standard method followed by a blank subtraction using the NexION software version 1.5 (Perkin Elmer, Waltham, MA, USA). The zinc concentration within the samples was determined based on an external calibration curve (0, 290, 580, 1,160 and 2,320 µg/L). As controls, VIM-2 protein without inhibitor, buffer control and diluent blanks for control of instrumental carry over and one sample for quality control of the measurements (580 µg/L standard) were included.

Liquid chromatography-electrospray ionisation Q-TOF mass spectrometry (LC-ESI-MS): VIM-2 (8 µM final concentration) was incubated together without or with 5 mM ZN148 on ice for 30 min. Incubation was carried out in chelex HEPES buffer, pH 7.5 and the inhibitor were diluted in Milli-Q water (Millipore/Merck, Darmstadt, Germany) by a factor of 1,000,000 using centrifugal filters (10,000 Da, Merck, Darmstadt, Germany). LC-ESI-MS (Agilent Technologies, Santa Clara, CA, USA) was performed in positive ion mode using formic acid 0.1% in Milli-Q water and acetonitrile (VWR, Radnor, USA) and 0.4 mL/min. Spectra deconvolution was performed by using BioConfirm and MassHunter Qualitative Analysis (Agilent Technologies, Santa Clara, CA, USA).

Reversibility and zinc restoration of enzyme activity:

For reversibility of enzyme activity after incubation with ZN148, 3 mL VIM-2 or NDM-1 were diluted with and without ZN148 in chelex HEPES buffer, pH 7.5 and subsequently incubated for 1 h on ice. 2.5 mL of each solution was loaded on an equilibrated PD-10 column (GE Healthcare, Pittsburg, PA, USA), washed with 1 mL and eluted with 1.5 mL chelex HEPES buffer, pH 7.5, respectively. Samples spiked and non-spiked with inhibitor were diluted to a final enzyme concentration of 1 nM VIM-2 and 3 nM NDM-1. The initial reaction velocity was determined by adding nitrocefin (Merck, Darmstadt, Germany) for VIM-2 or imipenem (Sigma Aldrich, St. Louis, USA) for NDM-1 at a final concentration of 50 µM and 100 µM, respectively. The initial enzyme reactions were recorded at 25°C. Inhibitor and enzyme alone were included as controls. All measurements were performed at least in duplicates. For enzyme restorability, pre- and post-column samples were supplemented with $ZnSO_4$ (Sigma Aldrich, St. Louis, USA) to a final concentration of 100 µM and allowed incubate for 5 min at 25°C and the initial enzyme velocity was determined as described above.

Un- and refolding of VIM-2:

VIM-2 (0.4 µM) was pre-incubated on ice for 30 min with and without ZN148. Complete protein unfolding was archived in 50 mM HEPES buffer, pH 7.5 supplemented with 1 µM $ZnSO_4$ (Sigma Aldrich, St. Louis, USA) and 8 M urea (Merck, Darmstadt, Germany). Refolding was achieved by a step-wise buffer exchange using centrifugal cut-off filters (Merck, Darmstadt, Germany, 10 kDa) and decreasing concentrations of urea (0, 2, 4 and 6 M in 50 mM HEPES buffer, pH 7.5). VIM-2 was diluted to a final concentration of 1 nM and the enzyme activity was measured by adding nitrocefin (Merck, Darmstadt, Germany) to a final concentration of 50 µM.

Modelling of ZN148 into VIM-2 and NDM-1:

ZN148 was modelled into VIM-2 and NDM-1 based on x-ray crystallography data of VIM-7 co-crystallized with ZN222 (C. Froelich and H-K. S. Leiros et al. unpublished), the protein-inhibitor/substrate complex structures of VIM-2 with triazolylthioacetamide (PDB ID: 5LSC) and NDM-1 bound to cefuroxime (PDB ID: 4RL0) by using Phenix version 1.12 (58). The 2-Pyridinyl rings in ZN148 were first placed at the same sites as for ZN222, and then the linker of the inhibitor was exiting the active site towards W87, N233 and residue 119 similar to the inhibitor triazolylthioacetamide in VIM-2 (PDB ID: 5LSC).

Acknowledgments:

We acknowledge the contribution of Ida Kristine Østnes Hansen at the UiT The Arctic University of Norway for performing the ESI-MS measurements. *In vivo* efficacy studies were performed at Statens Serum Institut, Copenhagen, Denmark and we are grateful for the support from Carina Vingsbo Lundberg. The *in vivo* tolerance study was performed by Antineo, France and part of the antimicrobial susceptibility testing was performed by IHMA Europe Sàrl, Switzerland. The whole genome sequencing was performed at the Norwegian Sequencing Centre.

Funding:

We thankfully acknowledge funding from The Research Council of Norway (BIOTEK2021 program, project no. 244219 and FORNY program, project no. 273430), NOVO Pre Seed

(NOVO Nordisk Fonden ByGS/SSch), Statoil AS (now Equinor AS) the University of Oslo and the Northern Norway Regional Health Authority (project no. SFP886-09). The funders had no role in study design, data collection and interpretation, or the decision to submit the work for publication.

Author contributions:

O.A.H.Å., A.B., and P.R. conceived and initiated the project; Ø.S., O.A.H.Å., C.F., A.H., H-K.S.L., S.S., A.B., T.G., O.A.Ø., and P.R. conceived and designed experimental methodology; O.A.H.Å., C.S., G.K-A., performed chemical synthesis; C.F., and S.L., performed antimicrobial susceptibility testing; A.H., S.F., O.A.Ø., performed *in vitro* time-kill experiments, frequency of resistance, serial passaging experiments and whole-genome sequencing; C.F., T.G., and A.M.S.A., performed *in vitro* toxicity studies; S.S., and T.J.O.C., performed recombinant expression and purification of VIM-2 and NDM-1; C.F. performed *in vitro* kinetic and mode of action experiments; H-K.S.L., and C.F. performed molecular modelling; S.H., and C.F., performed ICP-MS analysis; all authors analyzed, interpreted and contextualized the data; Ø.S., O.A.H.Å., and C.F. wrote the initial draft; All authors contributed to the final version.

Competing interests:

P.R, O.A.H.Å, Ø.S, C.S, G.K-A have a patent application on the technology (WO 2018033719 A1). All other authors declare no competing interests.

References:

1. Papp-Wallace KM, Endimiani A, Taracila MA, Bonomo RA. 2011. Carbapenems: past, present, and future. Antimicrob Agents Chemother 55(11):4943-60.
2. Bush K. The ABCD's of β-lactamase nomenclature. 2013. J Infect Chemother 19(4):549-59.
3. Logan LK, Weinstein RA. The epidemiology of carbapenem-resistant Enterobacteriaceae: the impact and evolution of a global menace. 2017. J Infect Dis 215(suppl_1):S28-S36.
4. Temkin E, Fallach N, Almagor J, Gladstone BP, Tacconelli E, Carmeli Y, DRIVE-AB Consortium. 2018. Estimating the number of infections caused by antibiotic-resistant *Escherichia coli* and *Klebsiella pneumoniae* in 2014: a modelling study. Lancet Glob Health. 6(9):e969-e79.
5. Cassini A, Hogberg LD, Plachouras D, Quattrocchi A, Hoxha A, Simonsen GS, Colomb-Cotinat M, Kretzschmar ME, Devleesschauwer B, Cecchini M, Ouakrim DA, Oliveira TC, Struelens MJ, Suetens C, Monnet DL, Burden of AMR Collaborative Group. 2019. Attributable deaths and disability-adjusted life-years caused by infections with antibiotic-resistant bacteria in the EU and the European Economic Area in 2015: a population-level modelling analysis. Lancet Infect Dis 19(1):56-66.
6. Perez F, El Chakhtoura NG, Papp-Wallace KM, Wilson BM, Bonomo RA. 2016. Treatment options for infections caused by carbapenem-resistant Enterobacteriaceae: can we apply "precision medicine" to antimicrobial chemotherapy? Expert Opin Pharmacother 17(6):761-81.
7. Zhanel GG, Lawrence CK, Adam H, Schweizer F, Zelenitsky S, Zhanel M, Lagacé-Wiens PRS, Walkty A, Denisuik A, Golden A, Gin AS, Hoban DJ, Lynch 3rd JP, Karlowsky JA. 2018. Imipenem-relebactam and meropenem-vaborbactam: two novel carbapenem-β-lactamase inhibitor combinations. Drugs 78(1):65-98.
8. Wright H, Bonomo RA, Paterson DL. New agents for the treatment of infections with Gram-negative bacteria: restoring the miracle or false dawn? 2017. Clin Microbiol Infect 23(10):704-12.
9. European Centre for Disease Prevention and Control. Regional outbreak of New Delhi metallo-β-lactamase producing carbapenem-resistant Enterobacteriaceae, Italy, 2018–2019 – 4 June 2019. ECDC: Stockholm; 2019.
10. Zhanel GG, Golden AR, Zelenitsky S, Wiebe K, Lawrence CK, Adam HJ, Idowu T, Domalaon R, Schweizer F, Zhanel MA, Lagacé-Wiens PRS, Walkty AJ, Noreddin A, Lynch 3rd JP, Karlowsky JA. Cefiderocol: a siderophore cephalosporin with activity against carbapenem-resistant and multidrug-resistant Gram-negative bacilli. 2019. Drugs. 79(3):271-89.
11. Chew KL, Tay MKL, Cheng B, Lin RTP, Octavia S, Teo JWP. 2018. Aztreonam-avibactam combination restores susceptibility of aztreonam in dual-carbapenemase-producing Enterobacteriaceae. Antimicrob Agents Chemother 62:e00414-18.
12. Emeraud C, Escaut L, Boucly A, Fortineau N, Bonnin RA, Naas T, Dortet L. 2019. Aztreonam plus clavulanate, tazobactam, or avibactam for treatment of infections caused by metallo-β-lactamase-producing Gram-negative bacteria. Antimicrob Agents Chemother 63:e00010-19.
13. Moya B, Barcelo IM, Cabot G, Torrens G, Palwe S, Joshi P, Umarkar K, Takalkar S, Periasamy H, Bhagwat S, Patel M, Bou G, Oliver A. 2019. *In vitro* and *in vivo* activities of β-lactams in combination with the novel β-lactam enhancers zidebactam and WCK 5153 against

multidrug-resistant metallo-β-lactamase-producing *Klebsiella pneumoniae*. Antimicrob Agents Chemother 63:e00128-19.
14. Mushtaq S, Vickers A, Woodford N, Haldimann A, Livermore DM. 2019. Activity of nacubactam (RG6080/OP0595) combinations against MBL-producing Enterobacteriaceae. J Antimicrob Chemother 74(4):953-60.
15. King AM, Reid-Yu SA, Wang W, King DT, De Pascale G, Strynadka NC, Walsh TR, Coombes BK, Wright GD. 2014. Aspergillomarasmine A overcomes metallo-β-lactamase antibiotic resistance. Nature. 510(7506):503-6.
16. Chen AY, Thomas PW, Stewart AC, Bergstrom A, Cheng Z, Miller C, Bethel CR, Marshall SH, Credille CV, Riley CL, Page RC, Bonomo RA, Crowder MW, Tierney DL, Fast W, Cohen SM. 2017. Dipicolinic acid derivatives as inhibitors of New Delhi metallo-β-lactamase-1. J Med Chem 60(17):7267-83.
17. Everett M, Sprynski N, Coelho A, Castandet J, Bayet M, Bougnon J, Lozano C, Davies DT, Leiris S, Zalacain M, Morrissey I, Magnet S, Holden K, Warn P, De Luca F, Docquier J-D, Lemonnier M. 2018. Discovery of a novel metallo-β-lactamase inhibitor that potentiates meropenem activity against carbapenem-resistant *Enterobacteriaceae*. Antimicrob Agents Chemother 62:e00074-18.
18. Hinchliffe P, Gonzalez MM, Mojica MF, Gonzalez JM, Castillo V, Saiz C, Kosmopoulou M, Tooke CL, Llarrull LI, Mahler G, Bonomo RA, Vila AJ, Spencer J. 2016. Cross-class metallo-β-lactamase inhibition by bisthiazolidines reveals multiple binding modes. Proc Natl Acad Sci U S A 113(26):E3745-54.
19. Wang R, Lai TP, Gao P, Zhang H, Ho PL, Woo PC, Ma G, Kao RY-T, Li H, Sun H. 2018. Bismuth antimicrobial drugs serve as broad-spectrum metallo-β-lactamase inhibitors. Nat Commun 9(1):439.
20. Hamrick JC, Docquier J-D, Uehara T, Myers CL, Six DA, Chatwin CL, John KJ, Vernacchio SF, Cusick SM, Trout REL, Pozzi C, De Luca F, Benvenuti M, Mangani S, Liu B, Jackson RW, Moeck G, Xerri L, Burns CJ, Pevear DC, Daigle DM. 2020. VNRX-5133 (taniborbactam), a broad-spectrum inhibitor of serine- and metallo-β-lactamases, restores activity of cefepime in *Enterobacterales* and *Pseudomonas aeruginosa*. Antimicrob Agents Chemother 64:e01963-19.
21. World Health Organization. Antibacterial agents in clinical development: an analysis of the antibacterial clinical development pipeline, including tuberculosis. Geneva. 2017;WHO/EMP/IAU/2017.12.
22. Blackman A. 2005. The coordination chemistry of tripodal tetraamine ligands. Polyhedron 24(1):1-39.
23. Anderegg G, Hubmann E, Podder NG, Wenk F. 1977. Pyridine-Derivatives as Complexing Agents .11. Thermodynamics of Metal-Complex Formation with Bis[(2-Pyridyl)Methyl]-Amine, Tris[(2-Pyridyl)Methyl]-Amine and Tetrakis[(2-Pyridyl)Methyl]-Amine Helv Chim Acta 60(1):123-40.
24. Schnaars C, Kildahl-Andersen G, Prandina A, Popal R, Radix S, Le Borgne M, Gjøen T, Andresen AMS, Heikal A, Økstad OA, Fröhlich C, Samuelsen Ø, Lauksund S, Jordheim LP, Rongved P, Åstrand OAH. 2018. Synthesis and preclinical evaluation of TPA-based zinc chelators as metallo-β-lactamase inhibitors. ACS Infect Dis 4(9):1407-22.
25. Kildahl-Andersen G, Schnaars C, Prandina A, Radix S, Le Borgne M, Jordheim LP, Gjøen T, Andresen AMS, Lauksund S, Fröhlich C, Samuelsen Ø, Rongved P, Åstrand OAH.

2019. Synthesis and biological evaluation of zinc chelating compounds as metallo-β-lactamase inhibitors. Medchemcomm 10(4):528-37.
26. Prandina AR, Radix S, Le Borgne M, Jordheim LP, Bousfiha Z, Fröhlich C, Leiros, H-K.S, Samuelsen Ø, Frøvold, E, Rongved P, Åstrand OAH. 2019. Synthesis and biological evaluation of new dipicolylamine zinc chelators as metallo-β-lactamase inhibitors. Tetrahedron 75(11):1525-40.
27. European Committee for Antimicrobial Susceptiblity Testing. Breakpoint tables for interpretation of MICs and zone diameters. 2018;Version 8.1, http://www.eucast.org.
28. Meini MR, Gonzalez LJ, Vila AJ. 2013. Antibiotic resistance in Zn(II)-deficient environments: metallo-β-lactamase activation in the periplasm. Future Microbiol. 8(8):947-79.
29. Hancock RE, Brinkman FS. 2002. Function of *Pseudomonas* porins in uptake and efflux. Annu Rev Microbiol 56:17-38.
30. Lister PD, Wolter DJ, Hanson ND. 2009. Antibacterial-resistant *Pseudomonas aeruginosa*: clinical impact and complex regulation of chromosomally encoded resistance mechanisms. Clin Microbiol Rev 22(4):582-610.
31. Connolly JP, Gabrielsen M, Goldstone RJ, Grinter R, Wang D, Cogdell RJ, Walker D, Smith DGE, Roe AJ. 2016. A highly conserved bacterial D-serine uptake system links host metabolism and virulence. PLoS Pathog 12(1):e1005359.
32. Bahr G, Vitor-Horen L, Bethel CR, Bonomo RA, González LJ, Vila AJ. 2018. Clinical evolution of New Delhi metallo-β-lactamase (NDM) optimizes resistance under Zn(II) deprivation. Antimicrob Agents Chemother 62:e01849-17.
33. Andreini C, Banci L, Bertini I, Rosato A. 2006. Zinc through the three domains of life. J Proteome Res 5(11):3173-8.
34. Chasapis CT, Loutsidou AC, Spiliopoulou CA, Stefanidou ME. 2012. Zinc and human health: an update. Arch Toxicol 86(4):521-34.
35. Pettinati I, Brem J, Lee SY, McHugh PJ, Schofield CJ. 2016. The chemical biology of human metallo-β-lactamase fold proteins. Trends Biochem Sci 41(4):338-55.
36. Christopeit T, Albert A, Leiros HS. 2016. Discovery of a novel covalent non-β-lactam inhibitor of the metallo-β-lactamase NDM-1. Bioorg Med Chem 24(13):2947-53.
37. Bergstrom A, Katko A, Adkins Z, Hill J, Cheng Z, Burnett M, Yang H, Aitha M, Mehaffey MR, Brodbelt JS, Tehrani KHME, Martin NI, Bonomo RA, Page RC, Tierney DL, Fast W, Wright GD, Crowder MW. 2018. Probing the Interaction of Aspergillomarasmine A with metallo-β-lactamases NDM-1, VIM-2, and IMP-7. ACS Infect Dis 4(2):135-45.
38. Gardonio D, Siemann S. 2009. Chelator-facilitated chemical modification of IMP-1 metallo-β-lactamase and its consequences on metal binding. Biochem Biophys Res Commun 381(1):107-11.
39. Siemann S, Brewer D, Clarke AJ, Dmitrienko GI, Lajoie G, Viswanatha T. 2002. IMP-1 metallo-β-lactamase: effect of chelators and assessment of metal requirement by electrospray mass spectrometry. Biochim Biophys Acta. 1571(3):190-200.
40. Garcia-Saez I, Docquier JD, Rossolini GM, Dideberg O. 2008. The three-dimensional structure of VIM-2, a Zn-β-lactamase from *Pseudomonas aeruginosa* in its reduced and oxidised form. J Mol Biol 375(3):604-11.
41. Murray CI, Van Eyk JE. 2012. Chasing cysteine oxidative modifications: proteomic tools for characterizing cysteine redox status. Circ Cardiovasc Genet 5(5):591.
42. Ju LC, Cheng Z, Fast W, Bonomo RA, Crowder MW. 2018. The continuing challenge of metallo-β-lactamase inhibition: mechanism matters. Trends Pharmacol Sci 39(7):635-47.

43. Christopeit T, Carlsen TJ, Helland R, Leiros HK. 2015. Discovery of novel inhibitor scaffolds against the metallo-β-lactamase VIM-2 by surface plasmon resonance (SPR) based fragment screening. J Med Chem 58(21):8671-82.

44. Leiros HK, Skagseth S, Edvardsen KS, Lorentzen MS, Bjerga GE, Leiros I, Samuelsen Ø. 2014. His224 alters the R2 drug binding site and Phe218 influences the catalytic efficiency of the metallo-β-lactamase VIM-7. Antimicrob Agents Chemother 58(8):4826-36.

45. Tacconelli E, Carrara E, Savoldi A, Harbarth S, Mendelson M, Monnet DL, Pulcini C, Kahlmeter G, Kluytmans J, Carmeli Y, Ouellette M, Outterson K, Patel J, Cavaleri M, Cox EM, Houchens CR, Grayson ML, Hansen P, Singh N, Theuretzbacher U, Magrini N, WHO Pathogens Priority List Working Group. 2018. Discovery, research, and development of new antibiotics: the WHO priority list of antibiotic-resistant bacteria and tuberculosis. Lancet Infect Dis 18(3):318-27.

46. Payne DJ, Gwynn MN, Holmes DJ, Pompliano DL. 2007. Drugs for bad bugs: confronting the challenges of antibacterial discovery. Nat Rev Drug Discov 6(1):29-40.

47. Theuretzbacher U, Outterson K, Engel A, Karlen A. 2019. The global preclinical antibacterial pipeline. Nat Rev Microbiol 10.1038/s41579-019-0288-0.

48. Clinical & Laboratory Standards Instiute. 2015. Methods for dilution antimicrobial susceptibility tests for bacteria that grow aerobically - Tenth Edition: Approved Standard M07-A10. CLSI, Wayne, PA, USA.

49. Heikal A, Samuelsen Ø, Kristensen T, Økstad OA. 2017. Complete genome sequence of a multidrug-resistant, *bla*$_{\text{NDM-1}}$-expressing *Klebsiella pneumoniae* K66-45 clinical isolate from Norway. Genome Announc 5:e00601-17.

50. Samuelsen Ø, Thilesen CM, Heggelund L, Vada AN, Kummel A, Sundsfjord A. Identification of NDM-1-producing Enterobacteriaceae in Norway. 2011. J Antimicrob Chemother 66(3):670-2.

51. Samuelsen Ø, Buaro L, Toleman MA, Giske CG, Hermansen NO, Walsh TR, Sundsfjord A. 2009. The first metallo-β-lactamase identified in Norway is associated with a TniC-like transposon in a *Pseudomonas aeruginosa* isolate of sequence type 233 imported from Ghana. Antimicrob Agents Chemother 53(1):331-2.

52. Miles AA, Misra SS, Irwin JO. 1938. The estimation of the bactericidal power of the blood. J Hygiene 38(6):732-49.

53. Livermore DM, Mushtaq S, Barker K, Hope R, Warner M, Woodford N. 2012. Characterization of β-lactamase and porin mutants of Enterobacteriaceae selected with ceftaroline + avibactam (NXL104). J Antimicrob Chemother 67(6):1354-8.

54. Langmead B, Salzberg SL. Fast gapped-read alignment with Bowtie 2. 2012. Nat Meth 9(4):357-9.

55. Kearse M, Moir R, Wilson A, Stones-Havas S, Cheung M, Sturrock S, Buxton S, Cooper A, Markowitz S, Duran C, Thierer T, Ashton B, Meintjes P, Drummond A. 2012. Geneious Basic: an integrated and extendable desktop software platform for the organization and analysis of sequence data. Bioinformatics 28(12):1647-9.

56. O'Brien J, Wilson I, Orton T, Pognan F. 2000. Investigation of the Alamar Blue (resazurin) fluorescent dye for the assessment of mammalian cell cytotoxicity. Eur J Biochem 267(17):5421-6.

57. Lund BA, Leiros HK, Bjerga GE. 2014. A high-throughput, restriction-free cloning and screening strategy based on *ccdB*-gene replacement. Microbial Cell Fact 13(1):38.

Antimicrobial Agents and Chemotherapy

58. Adams PD, Afonine PV, Bunkoczi G, Chen VB, Davis IW, Echols N, Headd JJ, Hung L-W, Kapral GJ, Grosse-Kunstleve RW, McCoy AJ, Moriarty NW, Oeffner R, Read RJ, Richardson DC, Richardson JS, Terwilliger TC, Zwart PH. 2010. PHENIX: a comprehensive Python-based system for macromolecular structure solution. Acta Crystallogr D Biol Crystallogr 66(Pt 2):213-21.

Figure legends:

Fig. 1: Chemical structure of ZN148

Fig. 2: Antimicrobial activity of carbapenem-ZN148 combinations. (A) Cumulative meropenem (MEM) minimum inhibitory concentration (MIC) alone or in combination with 50 µM ZN148 against MBL-producing *E. coli* (*n*=112), *K. pneumoniae* (*n*=112) and other *Enterobacterales* (*n*=10) and all strains (*n*=234) combined. (B) Cumulative doripenem (DOR) and imipenem (IPM) minimum inhibitory concentration (MIC) alone or in combination with 50 µM ZN148, against MBL-producing *E. coli* (*n*=87) and MBL-producing *K. pneumoniae* (*n*=85). (C) Cumulative meropenem (MEM), doripenem (DOR) and imipenem (IPM) minimum inhibitory concentration (MIC) alone or in combination with 50 µM ZN148, against MBL-producing *P. aeruginosa*. For MEM the collection included 61 strains, while for DOR and IPM the collection included 52 strains.

Fig. 3: Time-kill assay. NDM-1-producing *K. pneumoniae* K66-45 challenged with either meropenem (MEM) alone (4 mg/L, solid circles) or a combination of either 50 µM ZN148 plus MEM (4 mg/L, inverted open triangles) or 100 µM ZN148 plus MEM (4 mg/L, open triangles). Cell viability was expressed as $\log_{10}$ cfu/ml. Error bars represent the standard deviation from three independent technical replicates, limit of detection is indicated by the dotted line.

Fig. 4: *In vivo* activity of meropenem (MEM) and MEM-ZN148 combination. Neutropenic NMRI mice were inoculated intraperitoneally with ~$5x10^6$ CFU of NDM-1-producing *K. pneumoniae* 50752501 (MEM MIC = 64 mg/L). Mice were treated by subcutaneously injection in the neck region with vehicle (phosphate buffered saline), MEM (33 mg/kg) or MEM (33 mg/kg) + ZN148 (10 mg/kg). Vehicle and ZN148 were given one hour post-inoculation while MEM was given 1.5 hrs post-inoculation. Colony counts in blood (A) and peritoneal fluid (B)

762 were determined five hrs post-inoculation. Four mice were included in each group. Groups were
763 analyzed with ANOVA Dunnett´s multiple comparisons test and *P*-values <0.05 were considered
764 statistically significant.

765 **Fig. 5: Effect of ZN148 on human glyoxylase II and *in vivo* tolerance** (A) Enzyme activity of
766 recombinant human glyoxylase II in the presence of different concentrations of ZN148 (black
767 circles) and EDTA (grey circles). Error bars represent standard deviations. (B) *In vivo* tolerance
768 of ZN148 in female Balb/c mice (weekly intraperitoneal injection) compared to untreated
769 controls. Doses were doubled each week (4-128 mg/kg) in the absence of any observed weight
770 loss or modification in behaviour. Relative weight of mice in untreated (open circles) and
771 ZN148-treated (black squares) groups. Relative weight was calculated as the weight at the given
772 day divided by the weight at day 1. Data are mean values of 6 mice per group, and error bars
773 indicate the standard deviation.

774 **Fig. 6 Mode of action of ZN148** (A) Zinc content determination by ICP-MS of VIM-2 and
775 NDM-1 enzymes after pre-incubation with ZN148, demonstrating a removal of zinc from their
776 active sites. (B) Pre-incubation of VIM-2 with ZN148 (Pre PD10), the subsequent removal of the
777 inhibitor (Post PD10) and restoration of enzymatic activity by adding zinc (restoration) were
778 tested in order to describe the mode of inhibition. In contrast to EDTA, inhibition by ZN148 was
779 irreversible and activity could not be restored. (C) Un- and refolding of pre-incubated VIM-2
780 with ZN148 resulted in low enzyme activities. In contrast, un- and refolding of VIM-2 alone or
781 pre-incubated with EDTA demonstrated a refolding efficiency >80%. (D) ESI-MS of VIM-2 pre-
782 incubated with ZN148, revealing a change in mass of 46.2±0.1 Da. (E and F). Molecular
783 modelling of ZN148 (magenta) into VIM-2 (E) and NDM-1 (F). The modeling predicts aromatic
784 interactions between ZN148 and F61, Y67, Y224 and R228 in VIM-2 (E), which are unlikely in

785 NDM-1 due to the presence of M61, V67, K224 and A228 and where F63 is too far away for
786 aromatic stacking (F).

787

788

789 **Table legend:**

790 **TABLE 1**. Structures and kinetic properties of ZN148, ZN222, ZN223 and ZN228 against the
791 MBLs VIM-2 and NDM-1. K_I represents the inhibitor concentration that leads to half-maximum
792 inactivation, k_{inact} states the first-order rate constant and k_{inact}/K_I represents the catalytic
793 efficiency.

794

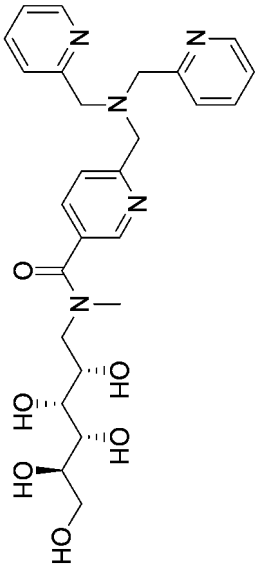

A

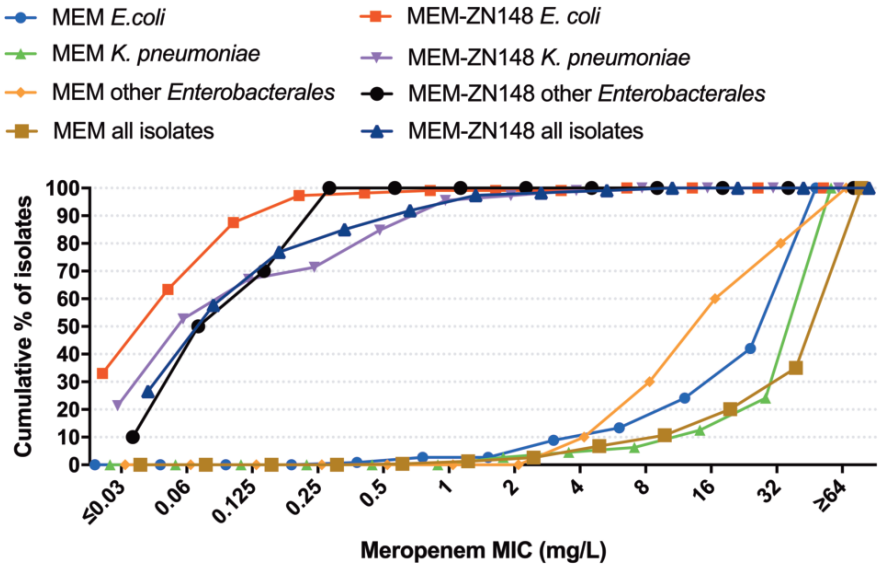

B

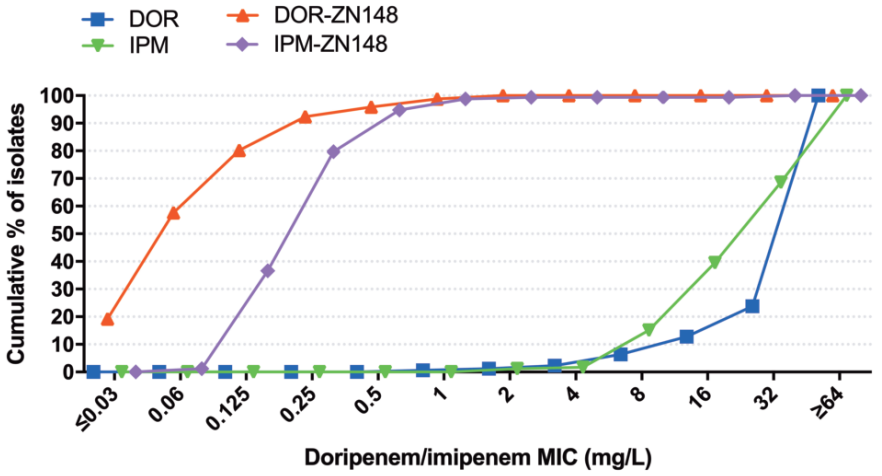

C

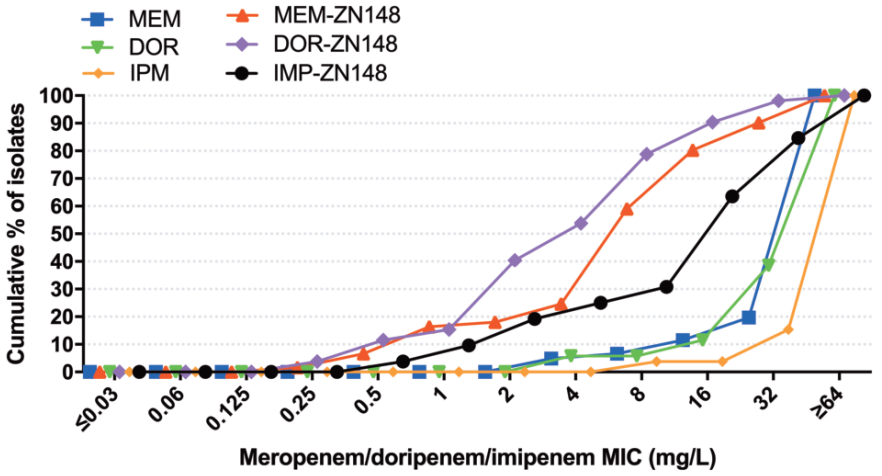

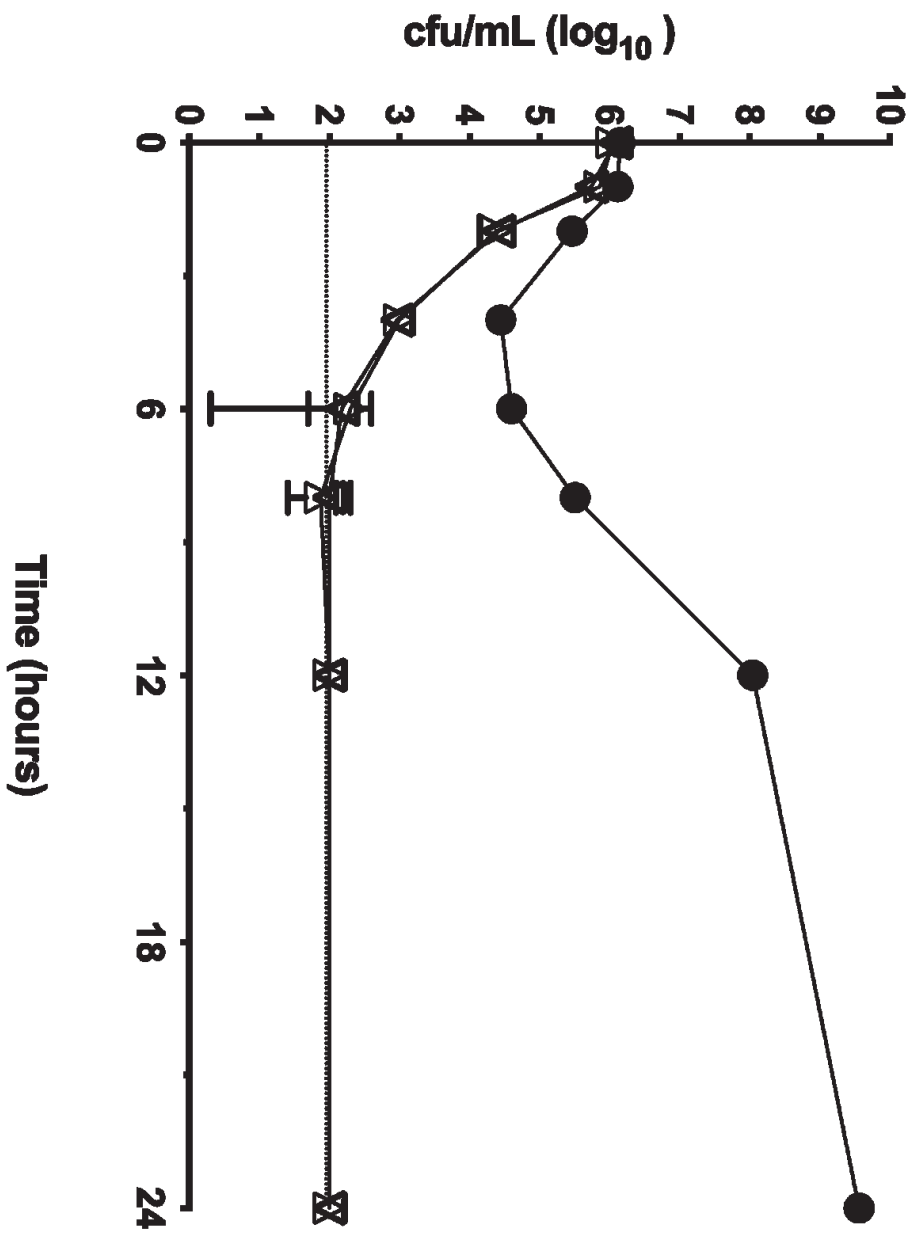

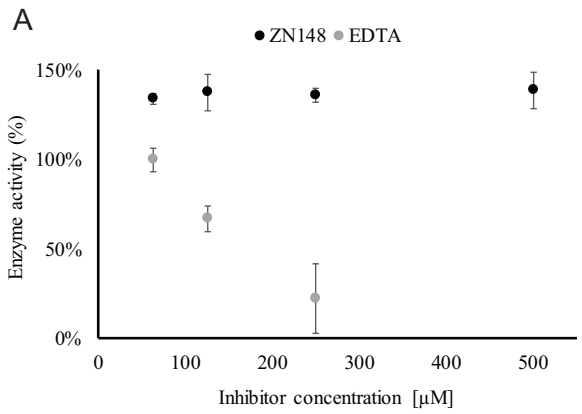

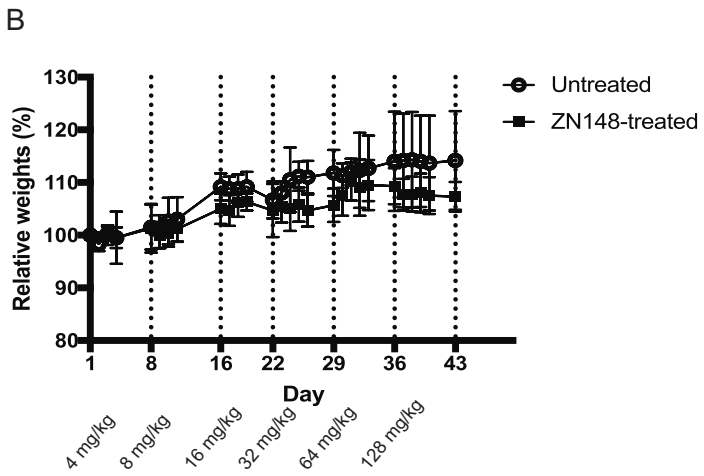

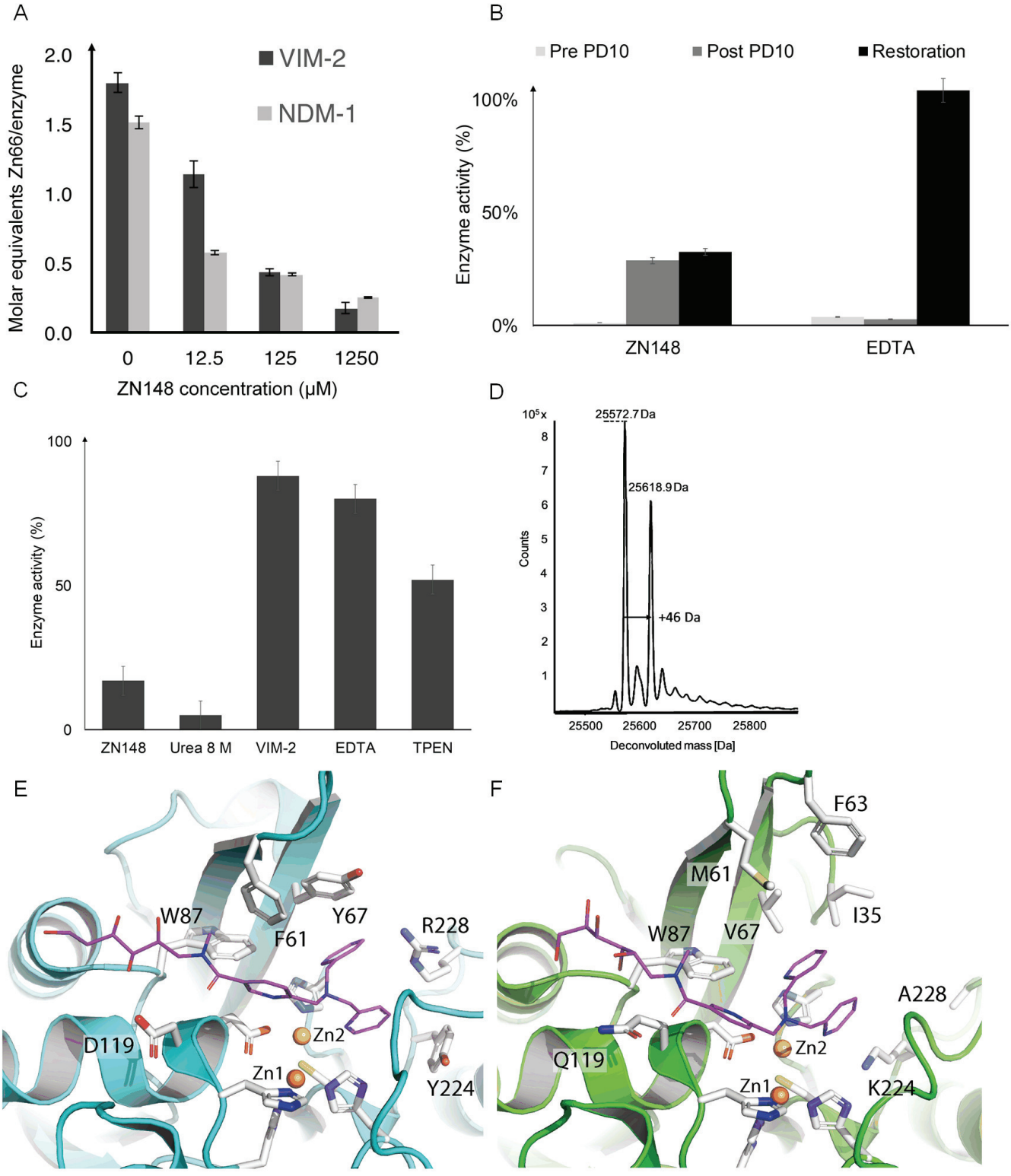

Compound	Structure	VIM-2			NDM-1		
		k_{inact} (min^{-1})	K_I (μM)	k_{inact}/K_I (min^{-1} mM^{-1})	k_{inact} (min^{-1})	K_I (μM)	k_{inact}/K_I (min^{-1} mM^{-1})
ZN148	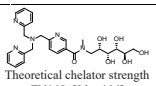 Theoretical chelator strength ZN148: Kd = 10^{-12}	0.157 ± 0.010	24 ± 3	6.6	0.059 ± 0.001	310 ± 13	0.19
ZN222	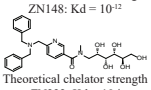 Theoretical chelator strength ZN222: Kd = 10^{-4}	NI	NI	NI	NI	NI	NI
ZN223	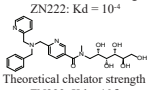 Theoretical chelator strength ZN223: Kd = 10^{-7}	0.037 ± 0.001	53 ± 4	0.7	0.038 ± 0.002	660 ± 56	0.06
ZN228	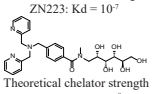 Theoretical chelator strength ZN228: Kd = 10^{-8}	0.034 ± 0.002	24 ± 6	1.4	0.076± 0.002	662 ±35	0.11

NI: no inhibition